

Enhanced giant magnetoimpedance effect and field sensitivity in Co-coated soft ferromagnetic amorphous ribbons

Nicholas Laurita,¹ Anurag Chaturvedi,¹ Christopher Bauer,¹ Priyanga Jayathilaka,¹ Alex Leary,² Casey Miller,¹ Manh-Huong Phan,^{1,a)} Michael E. McHenry,² and Hariharan Srikanth^{1,a)}

¹Department of Physics, University of South Florida, Florida 33620, USA

²Materials Science and Engineering Department, Carnegie Mellon University, Pittsburgh, PA 15213, USA

(Presented 16 November 2010; received 22 September 2010; accepted 8 November 2010; published online 22 March 2011)

A 50 nm-thick Co film has been grown either on the free surface (surface roughness, ~ 6 nm) or on the wheel-side surface (surface roughness, ~ 147 nm) of $\text{Co}_{84.55}\text{Fe}_{4.45}\text{Zr}_7\text{B}_4$ amorphous ribbons. A comparative study of the giant magnetoimpedance (GMI) effect and its field sensitivity (η) in the uncoated and Co-coated ribbons is presented. We show that the presence of the Co coating layer enhances both the GMI ratio and η in the Co-coated ribbons. Larger values for GMI ratio and η are achieved in the sample with Co coated on the free ribbon surface. The enhancement of the GMI effect in the Co-coated ribbons originates mainly from the reduction in stray fields due to surface irregularities and the enhanced magnetic flux paths closure. These findings provide good guidance for tailoring GMI in surface-modified soft ferromagnetic ribbons for use in highly sensitive magnetic sensors. © 2011 American Institute of Physics. [doi:10.1063/1.3548857]

The discovery of the so-called giant magnetoimpedance (GMI) effect in soft ferromagnetic ribbons makes them attractive for magnetic sensor applications.^{1,2} GMI is a large change in the ac impedance of a ferromagnetic conductor subject to a dc magnetic field.¹ The impedance (Z) of a ferromagnetic ribbon can be calculated by³

$$Z = R_{dc}jka \coth(jka), \quad (1)$$

where a is half of the thickness of the ribbon, R_{dc} is the electrical resistance for a dc current, $j = \text{imaginary unit}$, and $k = (1 + j)/\delta_m$. The impedance is related to the skin effect characterized by the skin depth (δ_m), which, in a magnetic medium, is given by

$$\delta_m = \sqrt{\frac{\rho}{\pi\mu_T f}}, \quad (2)$$

where ρ is the electrical resistivity, μ_T is the transverse magnetic permeability, and f is the frequency of the ac current. The application of a dc magnetic field H_{dc} changes μ_T , and consequently δ_m and Z . Since GMI is observed at high frequencies (>1 MHz), the skin effect is significant enough to confine the ac current to a sheath close to the surface of the conductor; GMI is therefore a surface-related magnetic phenomenon.^{2,3} As such, the surface roughness of a material is important and can considerably reduce the GMI magnitude if the surface irregularities exceed the skin depth.⁴⁻⁷ As an example, reducing the surface irregularities of Co-based amorphous ribbons by chemical polishing was found to greatly enhance the GMI effect.⁸ Peksoz *et al.* recently reported that the coating of the Co-based ribbon surface with CuO or a diamagnetic organic thin film improved the GMI

effect.^{9,10} While the origin of the enhanced GMI effect in the samples^{9,10} is not well understood, these investigations open up new opportunities for improving GMI effect in soft ferromagnetic ribbons.

We report here a comparative study of the GMI effect and its field sensitivity (η) in $\text{Co}_{84.55}\text{Fe}_{4.45}\text{Zr}_7\text{B}_4$ amorphous ribbons with and without 50 nm thick Co layers deposited on either the free ribbon surface (surface roughness, ~ 6 nm) or on the wheel-side ribbon surface (surface roughness, ~ 147 nm). This composition has a high Curie temperature compared to Fe-based amorphous alloys¹¹ and is responsive to field annealing.¹² We find a large enhancement of the GMI ratio and η in the Co-coated ribbons, both being largest in the sample with Co coated on the free ribbon surface. It is shown that the presence of the Co coating layer not only reduces stray fields due to surface irregularities, but also closes up the magnetic flux path, both of which contribute to the enhanced GMI effect in the Co-coated ribbons.

$\text{Co}_{84.55}\text{Fe}_{4.45}\text{Zr}_7\text{B}_4$ amorphous ribbons with a width of 2 mm and a thickness of 30 μm were prepared by the melt-spinning method.^{11,12} X-ray diffraction (XRD) confirmed the amorphous nature of the ribbons. The surfaces of the ribbons were then coated with 50 nm thick Co layers using magnetron sputtering. The surface morphology of the samples was analyzed using atomic force microscopy (AFM). We denote the free surface of the ribbon as that which had no contact with the surface of the copper wheel and the wheel-side ribbon surface as that which had direct contact with the surface of the copper wheel. Magnetic measurements were performed at room temperature using a vibrating sample magnetometer (VSM). Magnetoimpedance measurements in applied dc magnetic fields up to 120 Oe were carried out along the ribbon axis (1 cm long) over a frequency range of 0.1 \sim 10 MHz at a constant ac current of 5 mA using an impedance analyzer (HP4192A). The details of the measurement system have

^{a)}Electronic addresses: phanm@usf.edu and sharihar@usf.edu.

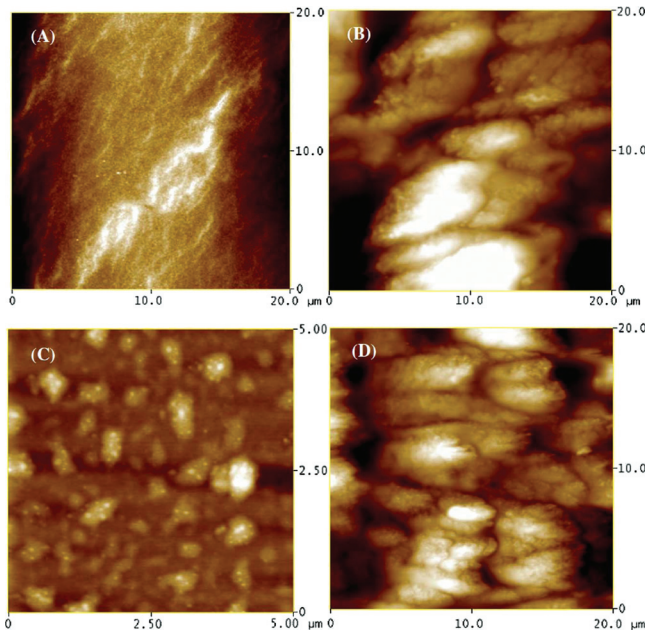


FIG. 1. (Color online) 2D topography images of (a) the free ribbon surface of the uncoated ribbon (Sample #1), (b) the wheel-side surface of the uncoated ribbon (Sample #2), (c) the free ribbon surface of the Co-coated ribbon (Sample #3), and (d) the wheel-side surface of the Co-coated ribbon (Sample #4).

been reported elsewhere.⁷ The GMI ratio and the magnetic field sensitivity of GMI ratio are defined as

$$\Delta Z/Z = 100\% \times \frac{Z(H) - Z(H_{\max})}{Z(H_{\max})} \quad (3)$$

and

$$\eta = \frac{d}{dH} \left(\frac{\Delta Z}{Z} \right), \quad (4)$$

where $Z(H)$ and $Z(H_{\max})$ represent the impedance in a magnetic field H and in the maximum field ($H_{\max} = 120$ Oe) respectively.

Figure 1 shows the AFM images of the surface topography of the uncoated and Co-coated ribbon samples for both surfaces. The AFM image indicates the distribution of protrusions with very high and uniform density for the free surface of the ribbon, unlike in the case of the wheel-side surface of the ribbon. The root mean squared (rms) surface roughness, $R_q = \frac{1}{n^2} \sqrt{\sum_{i=1}^n z_i^2}$, where z is the average amplitude of the topographical feature, was determined from the corresponding topographical data of Fig. 1 to be about 5.6 nm, 147 nm, 3.2 nm, and 61 nm for the free surface of the uncoated ribbon (Sample #1), the wheel-side surface of the uncoated ribbon (Sample #2), the free ribbon surface coated with Co (Sample #3), and the wheel-side ribbon surface coated with Co (Sample #4), respectively. Since Sample #1 and Sample #2 are both uncoated control samples, they have the same magnetic properties and GMI effect; we discuss below the M - H and GMI results of only samples #1, #3, and #4.

Figure 2 shows M - H loops taken at room temperature for samples #1, #3, and #4. The ribbon samples were 3 mm in length for these measurements. From the M - H data, the saturation magnetization (M_S) and the coercive field (H_c) are determined to be 120.5 emu/g and 7.0 Oe for Sample #1,

125.1 emu/g and 8.5 Oe for Sample #3, and 125.6 emu/g and 8.5 Oe for Sample #4. This indicates that the Co coating did not significantly change the static magnetic properties of the $\text{Co}_{84.55}\text{Fe}_{4.45}\text{Zr}_7\text{B}_4$ amorphous ribbons.

Figures 3(a) and 3(b) show the dc magnetic field dependence of GMI ratio ($\Delta Z/Z$) for samples #1, #3, and #4 at two representative frequencies, $f = 5$ MHz and 10 MHz. The frequency dependence of the maximum GMI ratio ($\Delta Z/Z_{\max}$) and the maximum field sensitivity of GMI (η_{\max}) of these samples are displayed in Figs. 3(c) and 3(d), respectively. It can be observed in Figs. 3(a) and 3(b) that a double-peak structure in the GMI profile is present for all samples investigated, with a more pronounced dip at zero field in Samples #3 and #4 than in Sample #1. From a sensor application perspective, it is very interesting to note that in the frequency range of 0.1 to 10 MHz, larger values of $(\Delta Z/Z)_{\max}$ and η_{\max} are achieved in Sample #3 and Sample #4 when compared to Sample #1. At $f = 2$ MHz, $(\Delta Z/Z)_{\max}$ and η_{\max} reach the largest values of 12.18% and 0.39%/Oe for Sample #1, 23.71% and 0.74%/Oe for Sample #3, and 17.85% and 0.50%/Oe for Sample #4. This clearly indicates that the Co coating enhances the GMI ratio and field sensitivity. Depositing the Co on the free ribbon surface with the smaller surface roughness ($R_q \sim 6$ nm) results in the larger $(\Delta Z/Z)_{\max}$ and η_{\max} when compared to that on the wheel-side ribbon surface with larger surface roughness ($R_q \sim 147$ nm). We have examined the effect of the Co coating on different ribbon samples and similar results are obtained (not shown here). Our findings are therefore of practical importance, demonstrating a way to tailor the GMI effect and field sensitivity in surface-modified ferromagnetic ribbons for use in highly sensitive magnetic sensors.

To explain the frequency dependence of $(\Delta Z/Z)_{\max}$ [Fig. 3(c)] and the enhancement of the GMI effect in these Co-coated ribbons [Figs. 3(c) and 3(d)], we have calculated the skin depth (δ_m) of the samples in the frequency range of 1 to 10 MHz using a simple relationship given by Kuzminski:¹³

$$\delta_m = a \frac{R_{\text{dc}}}{R_{\text{ac}}}, \quad (5)$$

where a is half of the ribbon thickness, R_{dc} is the dc resistance and R_{ac} is the ac resistance at a given frequency of the ac current. Figs. 4(a) and 4(b) show the frequency dependence of δ_m taken at $H_{\text{dc}} = 0$ Oe and Figs. 4(c) and (d) shows the frequency dependence of $\Delta \delta_m$ [$\Delta \delta_m = \delta_m(H_{\text{dc}} = 120 \text{ Oe}) - \delta_m(H_{\text{dc}} = 0)$]. From these results, the frequency dependence of $(\Delta Z/Z)_{\max}$ can be interpreted as follows: at frequencies below 1 MHz ($a < \delta_m$), $(\Delta Z/Z)_{\max}$ is relatively low due to the contribution of the induced magneto-inductive voltage to the measured magnetoimpedance.¹ In the range 1 MHz $\leq f \leq 2$ MHz ($a \approx \delta_m$), the skin effect is dominant, hence a higher $(\Delta Z/Z)_{\max}$ is observed. Above 2 MHz, $(\Delta Z/Z)_{\max}$ decreases with increasing frequency. This is because domain wall displacements are strongly damped due to eddy currents in this frequency regime, thus contributing less to the transverse permeability and $(\Delta Z/Z)_{\max}$. A similar explanation is also proposed for the frequency dependence of η_{\max} .

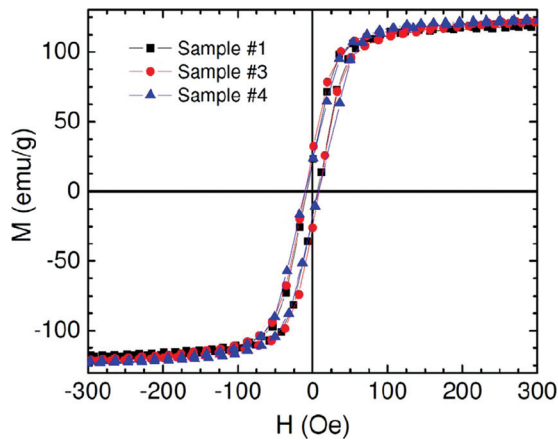


FIG. 2. (Color online) M - H loops taken at 300 K for Sample #1, Sample #3, and Sample #4.

On the origin of the enhanced GMI effect in the Co-coated ribbons, we recall that the surface roughness of the sample is important when the skin effect is strong.²⁻⁶ This is not only because the skin depth may become smaller than the surface irregularities, but also because stray fields that arise from rough surfaces cause a considerable reduction in the GMI magnitude.^{3,5,6} In the present case, the calculated values of δ_m [Fig. 4(a)] are much larger than the rms surface roughness of the ribbons determined from AFM ($R_q \sim 5.6 \times 10^{-3} \mu\text{m}$ for Sample #1, $3.2 \times 10^{-3} \mu\text{m}$ for Sample #3, and $61 \times 10^{-3} \mu\text{m}$ for Sample #4). However, stray fields arising from this surface effect may reduce GMI ratio at high frequencies.^{5,6} This can probably explain the larger values of $(\Delta Z/Z)_{\text{max}}$ and η_{max} in Sample #3 as compared to those of Sample #1 and Sample #4 for $f > 1$ MHz [see Figs. 3(c) and 3(d)]. An important feature to note is that although the δ_m is larger in Sample #3 and Sample #4 than in Sample #1 [Fig. 4(a)], the application of H_{dc} reduces δ_m to a greater extent (indicated by the larger values of $\Delta\delta_m$) in Sample #3 and Sample #4 [Fig. 4(b)]. Larger decreases in the reduced ac resistance (R/R_S) and the reduced reactance (X/X_S) with H_{dc} are also seen for

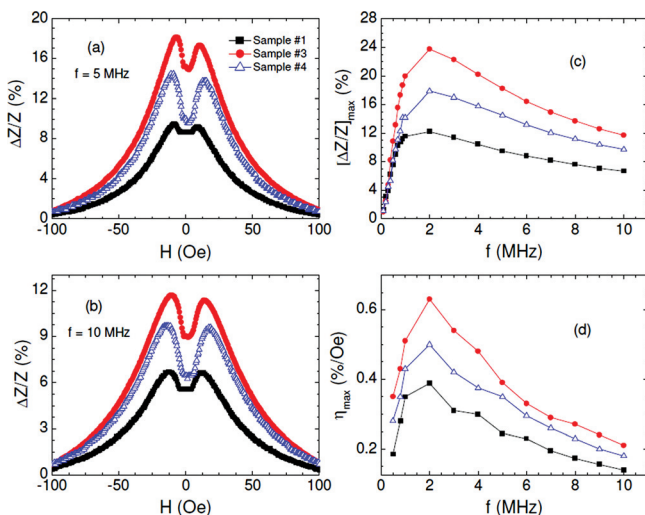


FIG. 3. (Color online) (a) and (b) Magnetic field dependence of GMI ratio ($\Delta Z/Z$) at 5 MHz and 10 MHz for Sample #1, Sample #3, and Sample #4; (c) and (d) Frequency dependence of the maximum GMI ratio ($\Delta Z/Z_{\text{max}}$) and the field sensitivity of GMI (η) for these samples.

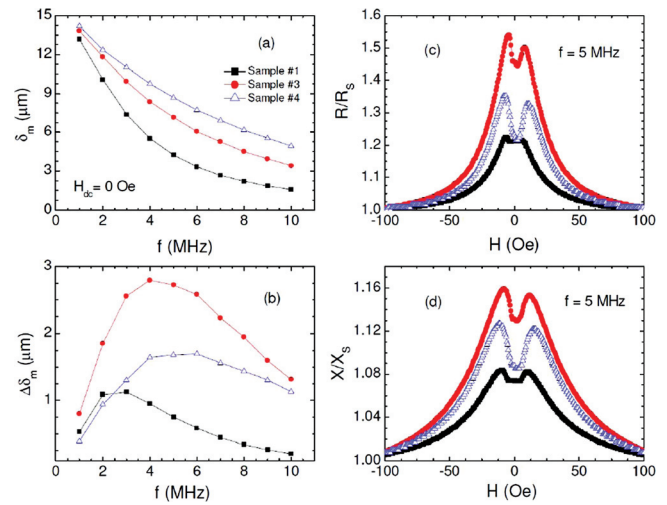


FIG. 4. (Color online) Frequency dependence of (a) the calculated skin depth δ_m and (b) $\Delta\delta_m = \delta_m(H_{\text{dc}} = 120 \text{ Oe}) - \delta_m(H_{\text{dc}} = 0)$ for Sample #1, Sample #3, and Sample #4. Magnetic field dependence of (c) the reduced resistance (R/R_S) and (d) the reduced reactance (X/X_S) for these samples.

Sample #3 and Sample #4, when compared to Sample #1 [Figs. 4(c) and (d)]. These results point to the important fact that the presence of the Co coating layer not only reduces stray fields due to surface irregularities,^{3,6} but also closes up the magnetic flux path,^{14,15} both of which are believed to lead to the enhancement of the GMI effect in Co-coated ribbons. The influence of Co coating on both sides of the ribbon on the GMI and field sensitivity is under investigation.

We have systematically studied the GMI effect and field sensitivity in $\text{Co}_{84.55}\text{Fe}_{4.45}\text{Zr}_7\text{B}_4$ amorphous ribbons with and without 50 nm thick Co coating layers. The presence of the Co coating layer enhances both the GMI effect and field sensitivity in the Co-coated ribbons. The largest values of GMI effect and field sensitivity are achieved in the sample coated with Co on the free ribbon surface, having a smaller surface roughness as compared to that coated with Co on the wheel-side ribbon surface with a larger surface roughness. Our studies demonstrate a method for tailoring the GMI effect and field sensitivity in surface-modified soft ferromagnetic ribbons for use in highly sensitive magnetic sensors.

The authors acknowledge support from USAMRMC through Grant No. W81XWH-07-1-0708 and the NSF through ECCS-0820880.

¹L. V. Panina, *et al.*, *IEEE Trans. Magn.* **31**, 1249 (1995).

²M. H. Phan and H. X. Peng, *Prog. Mater. Sci.* **53**, 323 (2008).

³L. Kraus, *Sens. Actuators A* **106**, 187 (2003).

⁴D. G. Park, *et al.*, *Physica B* **327**, 357 (2003).

⁵A. T. Le, *et al.*, *J. Magn. Magn. Mater.* **307**, (2006) 178.

⁶A. Chaturvedi, *et al.*, *Physica B* **405**, 2836 (2010).

⁷A. Chaturvedi, *et al.*, *Mater. Sci. Eng. B* **B172**, 146 (2010).

⁸F. Amalou and M. A. M. Gijs, *J. Appl. Phys.* **90**, 3466 (2001).

⁹A. A. Taysioglu, *et al.*, *J. Alloys Compd.* **487**, 38 (2009).

¹⁰A. Peksoz, *et al.*, *Sens. Actuators A* **A159**, 69 (2010).

¹¹P. R. Ohodnicki, *et al.*, *J. Appl. Phys.* **105**, 07A322 (2009).

¹²P. R. Ohodnicki, *et al.*, *J. Appl. Phys.* **104**, 113909 (2008).

¹³M. Kuzminski and H. K. Lachowicz, *J. Magn. Magn. Mater.* **267**, 35 (2003).

¹⁴F. Amalou and M. A. M. Gijs *Appl. Phys. Lett.* **81**, 1654 (2002).

¹⁵M. H. Phan, *et al.*, *J. Magn. Magn. Mater.* **316**, e253 (2007).